DOI: 10.1002/ejic.200900676

Rational, Facile Synthesis and Characterization of the Neutral Mixed-Metal Organometallic Oxides $Cp^*_2Mo_xW_{6-x}O_{17}$ ($Cp^* = C_5Me_5$, $x = 0, 2, 4, 6$)

Gülnur Taban-Çalışkan,[a,b,c] Dominique Agustin,*[a,b] Funda Demirhan,*[c] Laure Vendier,[a] and Rinaldo Poli*[a,d]

Keywords: Organometallic oxides / Tungsten / Molybdenum / Polyoxometalates / Density functional calculations / X-ray diffraction

The reaction of the bis(pentamethylcyclopentadienyl)pentaoxidodimetal complexes $Cp^*_2M_2O_5$ with four equivalents of $Na_2M'O_4$ (M, M′ = Mo, W) in acidic aqueous medium constitutes a soft and selective entry into neutral Lindqvist-type organometallic mixed-metal oxides $Cp^*_2Mo_xW_{6-x}O_{17}$ [x = 6 (**1**), 4 (**2**), 2 (**3**), 0 (**4**)]. The identity of the complexes is demonstrated by elemental analyses, thermogravimetric analyses and infrared spectroscopy. Thermal degradation of **1**–**4** up to above 500 °C leads to $Mo_{x/6}W_{1-x/6}O_3$. The molecular identity and geometry of compound **2** is further confirmed by a fit of the powder X-ray diffraction pattern with a model obtained from previously reported single-crystal X-ray structures of **1** and **4**, with which **2** is isomorphous. DFT calculations on models obtained by replacing Cp^* with Cp (**I**–**IV**) validate the structural assignments and assist in the assignment of the M,M′–O vibrations.

Introduction

Mixed oxides containing two or more different metals attract interest because of a number of different applications in heterogeneous catalysis[1–7] and in the elaboration of chromogenic materials,[8] the advantage being the tunability of the desired property (reactivity, light absorption, etc.) by modification of the nature and relative proportion of the different metals. A drawback is the difficulty to obtain materials with a homogeneous metal distribution at the atomic level by the currently applied techniques (sputtering, CVD).[9] For catalytic applications, the use of polyoxometalates (POMs) can provide a "molecular scale" model for a better understanding of the interaction between the substrates and the oxide surface.[10–12] For several decades, polyoxometallic species have attracted much interest because of their great versatility, with applications from biology to materials science and catalysis.[13] Numerous research groups worldwide are specialized in the synthesis of these molecules with fine control of shape, size and elemental composition.[13,14] One synthetic strategy employs the assembly of predefined polyatomic fragments, often performed in organic solvents and with air- and water-sensitive organometallic precursors.[13,15–20] Another method uses the grafting of simple organic fragments on lacunary oxo clusters.[14,21–29] Hydrothermal synthesis from elementary bricks is also an alternative, though limited by serendipity.[30,31] Some of these syntheses lead to heterometallic species but need to be performed in a specific environment, that is under argon or under pressure or with use of very sensitive species. Stability and/or compatibility with protic reagents and solvents are also useful for applications in "non-innocent" aqueous media. The introduction of organometallic moieties in a POM framework has attracted considerable attention,[13,32–38] because the organometallic fragment may impart new reactivity to the molecule relative to the all-inorganic equivalents. This strategy also allows the selective assembly of mixed-metal clusters under mild conditions, often using aqueous solvents. Specifically, the reaction of Na_2MO_4 (M = Mo, W) with $[Cp^*RhCl_2]_2$ or $[(\eta^6\text{-arene})RuCl_2]_2$ in water or acetonitrile yielded the octanuclear compounds $[(LM)(MoO)(\mu\text{-}O)_3]_4$ [LM = Cp^*Rh[32] and (*p*-MeC_4H_4iPr)Ru[33]] and their tungsten analogues $[(\{\eta^6\text{-arene}\}Ru)_4(WO)_4(\mu\text{-}O)_{12}]$ (arene = C_6Me_6, $pMeC_6H_4$-*i*Pr).[38]

[a] CNRS; LCC (Laboratoire de Chimie de Coordination), Université de Toulouse, UPS, INPT,
205, route de Narbonne, 31077 Toulouse, France
Fax: +33-5-61553003
E-mail: rinaldo.poli@lcc-toulouse.fr
[b] Université de Toulouse, Institut Universitaire de Technologie Paul Sabatier, Département de Chimie,
Av. Georges Pompidou, BP 20258, 81104 Castres Cedex, France
Fax: +33-5-63356388
E-mail: dominique.agustin@iut-tlse3.fr
[c] Celal Bayar University, Faculty of Sciences & Liberal Arts, Department of Chemistry,
45030 Muradiye-Manisa, Turkey
Fax: +90-02362412158
E-mail: funda.demirhan@bayar.edu.tr
[d] Institut Universitaire de France,
103, bd Saint-Michel, 75005 Paris, France
Supporting information for this article is available on the WWW under http://dx.doi.org/10.1002/ejic.200900676.

We have worked extensively on the aqueous chemistry of the air-stable organometallic complexes $Cp^*_2M_2O_5$ (M = Mo, W)[39–50] and have recently reported the synthesis and structure of $Cp^*_2Mo_6O_{17}$ (**1**).[51] This is a hexanuclear organopolyoxometallic species with a Lindqvist-type octahedral arrangement of the six Mo atoms, as shown in Scheme 1. Each Mo atom bears a terminal Cp* or oxido group, all edges of the octahedron are oxido-bridged, and there is an additional central (μ_6-O) atom bonded to all Mo centres, thus the formula can be written as $[(Cp^*Mo)_2(MoO)_4(\mu_2\text{-}O)_{12}(\mu_6\text{-}O)]$. It is isoelectronic with the $[Cp^*Mo_6O_{18}]^-$ and $[Mo_6O_{19}]^{2-}$ ions.[52–55] Small amounts of crystals suitable for a structural determination were obtained by a serendipitous slow decomposition of $Cp^*_2Mo_2O_5$ under strong acidic conditions, but the selective and high-yield synthesis was achieved by condensation of $Cp^*_2Mo_2O_5$ with four equivalents of Na_2MoO_4 under acidic conditions. The identity and purity of the microcrystalline powder was confirmed by comparison of the X-ray powder diffraction spectrum with that simulated from the single-crystal data. On the basis of this finding, we set out to extend this strategy to the full series of $[(Cp^*M)_2(M'O)_4(\mu_2\text{-}O)_{12}(\mu_6\text{-}O)]$ complexes in which M,M′ = Mo, W, to include the previously unknown mixed-metal species. The M = M′ = W compound, $Cp^*_2W_6O_{17}$, has previously been described but was only obtained as a "major oxidation product" from a sealed-tube reaction between $[Cp^*W(CO)_2]_2$ and the arsaoxane impurity in the cyclic polyarsine *c*-$(AsCH_3)_5$ as oxygen-transfer agent.[56] As described herein, the same synthetic protocol leads to the full series of $Cp^*_2M_2M'_4O_{17}$ compounds.

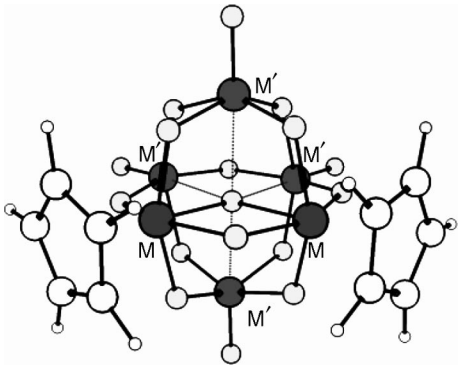

Scheme 1. Structure of the $[(Cp^*M)_2(M'O)_4(\mu_2\text{-}O)_{12}(\mu_6\text{-}O)]$ compounds (M, M′ = Mo, W).

Results and Discussion

Synthesis

The reaction between $Cp^*_2M_2O_5$ and $M'O_4^{2-}$ (M, M′ = Mo, W), under the conditions previously described for the synthesis of the Mo_6 derivative **1**,[51] affords all other three complexes in excellent yields and purity [see Equation (1)].

$$Cp^*_2M_2O_5 + 4\ M'O_4^{2-} + 8\ H^+ \rightarrow Cp^*_2M_2M'_4O_{17} + 4\ H_2O \quad (1)$$

Compound	M	M'
1	Mo	Mo
2	W	Mo
3	Mo	W
4	W	W

Mixing a methanol solution of $Cp^*_2M_2O_5$ (this compound is insoluble in pure water but soluble in aqueous methanol solutions) and an aqueous solution of $Na_2M'O_4$ (4 equiv.) yields the products as fine precipitates immediately after acidification. The colour of the compound varies from orange-brown to yellow-green, depending on the Mo/W ratio. Direct contact with metallic materials (i.e. syringe needles or spatulas) causes reduction with strong darkening of the compound's colour towards green and should therefore be avoided.

Previous work in our group has shown that the Cp*–Mo bond in $Cp^*_2Mo_2O_5$ is quite robust and withstands exposure to aqueous media in the entire pH range, at least for reasonably long periods of time.[39] Analogous studies for the W analogue have not been carried out, but W–ligand bonds are usually stronger than those of the Mo congeners. Thus, it is not surprising that the Cp*M moieties are transferred intact from the $Cp^*_2M_2O_5$ starting materials to the products. Our previous studies have also shown that $Cp^*_2Mo_2O_5$ ionizes in water and yields the species $Cp^*MoO_2^+$ and $Cp^*MoO_2(H_2O)^+$ at low pH.[39,57] Once again, the behaviour of the W analogue under the same conditions has not been investigated but can be assumed to parallel that of Mo. Thus, the synthesis can be seen as the assembly of individual organometallic $Cp^*MO_2^+$ and inorganic $M'O_4^{2-}$ species, regulated by stoichiometry and pH. The products are stable in water at low pH. Upon raising the pH, however, the solid redissolves in the medium, slowly at pH 6, faster at higher pH, possibly regenerating a mixture of the starting materials (the formation of $Cp^*_2Mo_2O_5$ was confirmed by IR on the isolated residue). Unfortunately, the compounds are insufficiently soluble in common solvents for characterization by techniques such as NMR or electrochemistry, but they could be characterized by solid-state analytical methods (IR, TGA and powder X-ray diffraction, vide infra)

DFT Calculations

DFT geometry optimizations were carried out for the purpose of assigning the IR absorption bands and interpreting the effect of the metal on them. To save computational time, the calculations were run on simplified models (indicated by roman numerals corresponding to the numbering scheme of the compounds) where the Cp* ligands were replaced by Cp rings. Before examining these results, we present a brief description of the optimized geometries. The results are collected in Table 1. Since the four M′ atoms occupy structurally distinct positions, we shall distinguish

Table 1. Selected bond distances [Å] for the geometry optimized models **I**–**IV** and comparison with the experimental structures of **1** and **4**.[a]

System (M, M′ = M′′)	**1**[b] (Mo, Mo)	**I** (Mo, Mo)	**II** (W, Mo)	**III** (Mo, W)	**IV** (W, W)	**4**[c] (W, W)
Cp–M	2.109(5)	2.13	2.14	2.12	2.13	2.11(4)
M′=O_t	1.687(3)	1.68	1.68	1.69	1.69	1.69(2)
M′′=O_t	1.683(3)	1.68	1.68	1.70	1.70	1.69(2)
M–O_c	2.145(2)	2.13	2.12	2.15	2.14	2.20(1)
M′–O_c	2.542(3)	2.62	2.62	2.60	2.61	2.50(2)
M′′–O_c	2.3674(5)	2.41	2.41	2.39	2.39	2.36(2)
M–$O_{b(M)}$	1.943(2)	1.95	1.95	1.95	1.94	1.93(1)
M–$O_{b(M′)}$	1.955(3)	1.92	1.92	1.93	1.92	1.94(2)
M–$O_{b(M′′)}$	2.029(3)	2.04	1.99	1.95	1.94	1.97(2)
	1.890(3)	1.86	1.88	1.93	1.93	1.92(2)
M′–$O_{b(M)}$	1.883(3)	1.93	1.93	1.92	1.92	1.89(2)
M′–$O_{b(M′)}$	1.916(2)	1.91	1.91	1.92	1.91	1.92(1)
M′–$O_{b(M′′)}$	1.977(3)	2.00	1.99	1.93	1.92	1.93(2)
	1.861(3)	1.86	1.86	1.92	1.92	1.92(2)
M′′–$O_{b(M)}$	1.980(3)	2.02	1.89	1.93	1.94	1.93(2)
	1.855(3)	1.86	2.00	1.94	1.94	1.92(2)
M′′–$O_{b(M′)}$	2.006(3)	2.01	1.99	1.93	1.92	1.94(2)
	1.871(3)	1.86	1.87	1.92	1.92	1.94(2)

[a] For the definition of the symbols used, see Scheme 2. [b] From the X-ray structure published in ref.[51]. [c] From the X-ray structure published in ref.[56].

them by introducing the $M'_2M''_2$ notation, which will be limited to the structural description. The agreement between experimental and calculated geometries for the $M_2M'_2M''_2O_{17}$ core is generally very good, including the asymmetry of the M–O_b, M′–O_b and M′′–O_b distances, which is more pronounced for the Mo_6 structure but experimentally visible also in some of the W_6 structural parameters. The reason for this distortion is not clear, but the computational method seems to confirm that the distortion is a molecular phenomenon, not related to crystal packing. The molecules are located on a crystallographic twofold axis, as shown in Scheme 2, thus each pair of M′=O_t, M′′=O_t, M–O_c, M′–O_c and M′′–O_c bonds are equivalent by symmetry. Although the geometry optimizations were carried out without any symmetry constraints, this twofold symmetry was essentially maintained in the optimized geometries. The calculated distances to the terminal and bridging ligands are generally only slightly longer than those experimentally observed (maximum deviation 0.04 Å for M–$O_{M''}$ in **I**), whereas the distances to the central O atom are underestimated for M–O_c (by 0.01 Å in **I** and by 0.06 Å in **IV**) and overestimated for M′–O_c and M′′–O_c (by up to 0.11 Å in **IV**). Note that O_c is much closer to M than to M′ and M′′ and that the calculations tend to place O_c even closer to M relative to the experimental structure, which could be related to the use of the simplified model.

After establishing the suitability of this level of theory to reproduce the structural features, it is now interesting to examine some specific trends along the series of the optimized structures. The M′=O_t and M′′=O_t distances slightly lengthen on going from Mo to W. All distances to O_c, on the other hand, shorten on going from Mo to W. No clear trends can be established for the distances to the O_b atoms because of the asymmetry caused by the distortion from C_{2v} symmetry. It is also difficult to establish whether there

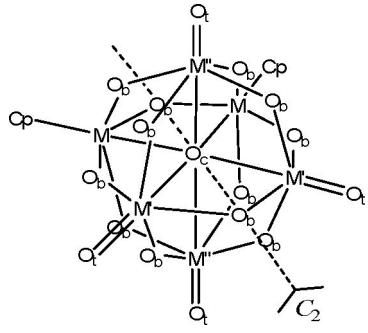

Scheme 2. Atom labelling scheme used in Table 1.

are secondary effects, for instance, of the nature of M′ and M′′ on the M–O_b distances. Going from Mo to W for M′ and M′′ seems to lead to M–O_c shortening, whereas no significant change is visible in the M′=O_t and M′′=O_t distances caused by changing the nature of M. Given the sensitivity of the DFT optimization procedure, we do not consider differences at the level of the third significant digit as reliable. Secondary effects will be more clearly revealed by the IR study.

IR Characterization

Infrared spectroscopy is a good characterization tool for polyanions, especially when they possess high symmetry, as in the case of $M_6O_{19}^{2-}$ Lindqvist anions (M = Mo, W).[58,59] The number of vibrations observed for salts of these anions agrees with the O_h space group, and a correlation between the experimental and calculated spectra could be established.[60] As already discussed above, the symmetry of systems **1**–**4** is reduced to C_2 (considering Cp* as a rapidly

rotating ligand), with an ideal C_{2v} symmetry if the M–O_b, M′–O_b and M′′–O_b asymmetry is averaged.

The observed (for **1**–**4**) and calculated (for **I**–**IV**) IR spectra in the metal–oxygen stretching region are shown in Figure 1, and the most prominent absorptions are listed in Tables 2 (calculated) and 3 (experimental). Views of the normal modes of vibrations corresponding to these calculated bands are available in the Supporting Information. The terminal M′=O_t and M′′=O_t vibrations are in the higher frequency part of the spectrum (observed: 950–1000 cm^{-1}; calculated: 1020–1050 cm^{-1}), whereas the vibrations involving the O_b atoms are in the 750–850 cm^{-1} range. A few Cp C–C in-plane and C–H out-of-plane bending motions are also present in this region (840–960 cm^{-1}) but have low intensity and do not significantly contribute to the calculated spectrum. The match between calculated and observed spectra is satisfactory, the frequency difference being related to the computational method, to the model (Cp vs. Cp*) or to a combination of both. The observed and calculated relative intensities, on the other hand, match rather well, giving us confidence in the assignment of the observed bands.

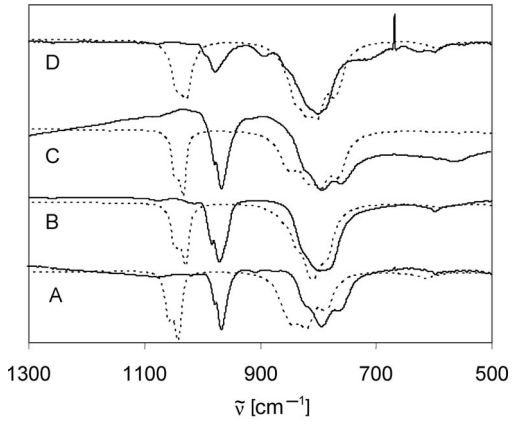

Figure 1. Experimental (solid lines) and calculated (DFT; unscaled, dotted lines) IR spectra in the Mo–O stretching region for compounds **1/I** (A), **2/II** (B), **3/III** (C), **4/IV** (D).

Table 3. Observed metal–O vibrations [cm^{-1}] in the 700–1100 cm^{-1} region.

1	2	3	4	Assignment
764m	780s	760s	789sh	ν[Mt–O–Mt]
794s	797s	793s	799s	ν[Mt–O–Mt]
820m	825sh	820sh	820sh	ν[Mt–O–Mt]
968s	971s	967s	977s	ν_{as}(M′′=O)
980m	984m	979m	994m	ν(M′=O)

We can now discuss with confidence the frequency trends related to each metal. First of all, the nature of the normal modes for the bands associated with the O_b atoms does not allow a fine analysis of the distortion from the ideal C_{2v} to the observed C_2 symmetry, thus the higher symmetry point group labels are used in Table 2 and in the discussion. Four terminal metal–oxido (M′=O_t and M′′=O_t) vibrations are expected and indeed calculated. One of them, ν_s(M′=O), is very weak because the two bonds are essentially collinear, and the overall dipole moment change is small. The small intensity is due to the deviation from collinearity and to a small vibrational coupling with the ν_s(M′=O) vibration, also of a_1 type (see Figure S1 in the Supporting Information). Thus, only three major bands are essentially observed in this region. The calculated frequencies show both a primary and a secondary effect. As M′ and M′′ go from Mo (**I/II**) to W (**III/IV**), all four frequencies experience a blueshift. However, a blueshift is also caused by the secondary effect of changing M from Mo (**I/III**) to W (**II/IV**). From the experimental spectra only two ν(M=O) bands can be unambiguously determined. Comparison with the calculated spectra suggest that the strongest one is ν_{as}(M′′=O), whereas the second smaller band is most probably the highest frequency a_1 band. The determination of the band positions is less accurate because of the broadening and resolu-

Table 2. Calculated metal–O vibrations [cm^{-1}] in the 700–1100 cm^{-1} region with relative intensities [km/mol] in parentheses.

Type[a]	**I**	**II**	**III**	**IV**	Assignment
b_1	770	786	766	785	ν_{as}[M–O–Mt][b]
	(723)	(879)	(803)	(927)	
a_1	801	807	795	809	ν_{as}[M–O–M′+M–O–M′′]
	(853)	(820)	(859)	(927)	
b_2	820	815	818	821	ν[Mt–O–Mt][b]
	(661)	(688)	(734)	(765)	
b_1	838	836	845	848	ν[Mt–O–Mt][b]
	(283)	(350)	(268)	(273)	
a_1	839	838	854	856	ν[Mt–O–Mt][b]
	(291)	(218)	(399)	(159)	
b_1	1027	1029	1033	1036	ν_{as}(M′′=O)
	(484)	(497)	(389)	(389)	
a_1	1030	1032	1036	1038	ν_s(M′=O) [–ν_s(M′=O)]
	(15)	(19)	(13)	(15)	
b_2	1038	1040	1042	1044	ν_{as}(M′=O)
	(212)	(213)	(163)	(163)	
a_1	1046	1048	1048	1050	ν_s(M′=O) [+ν_s(M′′=O)]
	(280)	(274)	(215)	(201)	

[a] Under idealized C_{2v} symmetry. [b] Mt = M, M′ and M′′.

tion, but the same trends for the calculated bands appears to be observed, the primary effect being most evident in the comparison of **2** with **4**, while the secondary effect is clearly evident in comparisons of **1** with **2** as well as **3** with **4**. The 12 metal–(bridging O atom) bonds yield in principle 12 normal modes, but only five of the six asymmetric motions can be clearly identified for the calculated spectrum (and three in the observed spectrum) in the typical "fingerprint region", while the symmetric motions are located at lower frequency and combined with other types of vibrations. These bands also shift to higher frequency when one or both metals directly implicated in the bond(s) is (are) changed from Mo to W. Experimentally, the most significant change in this region is seen as a result of changing the inorganic metal, whereas changing the organometallic one produces hardly any effect. For the a_1 ν[Mt–O–Mt] band, to which the main contributions come from M′ and M′′, the secondary effect of changing M is small. All other observed bands involve a combination of M–O_b on one side and M′–O_b or M′′–O_b on the other side, thus a distinction of primary and secondary effects is not possible.

TGA Measurements

Upon warming up to 600 °C in thermogravimetric experiments conducted in air, all compounds undergo complete loss of their organic part, with a good match between experimentally observed and theoretical mass losses on the basis of Equation (2). The results of the TGA of compounds **1** and **3** are shown in Figure 2, while those of **2** and **4** are given in the Supporting Information. The onset of the Cp* ligand loss occurs at lower temperatures for **1** (190 °C) and **3** (230 °C), in which these ligands are bonded to Mo, whereas higher temperatures are necessary to induce loss of the Cp* bonded to W (270 °C for **2** and 310 °C for **4**). A secondary effect of the inorganic metal, however, is notable by comparing these temperatures for the couples **1/2** and **3/4**. Interestingly, the two Cp* rings are lost in two quite distinct and sharp steps for compound **1**, whereas a more gradual loss within a broader temperature range is observed for the other three compounds. The resulting residues from **1** and **4** had the expected colour (white for MoO_3, yellow for WO_3). The final product of the thermal decomposition of **2** and **3** is thus a mixed-metal oxide material with controlled metal composition, $Mo_{2/3}W_{1/3}O_3$ and $Mo_{1/3}W_{2/3}O_3$, respectively.

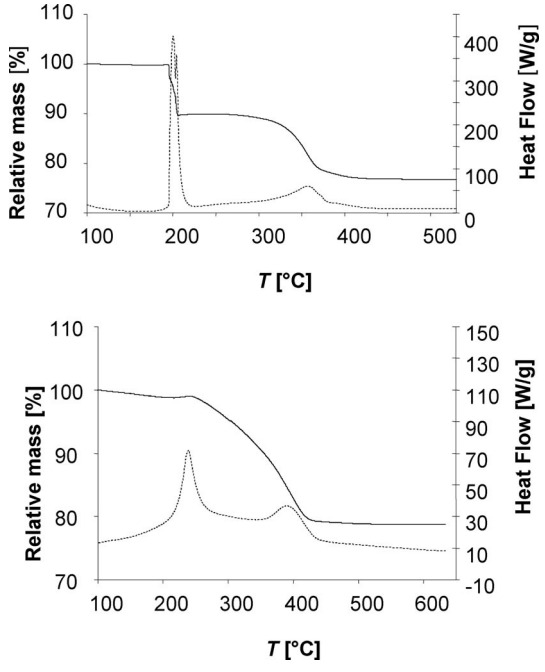

Figure 2. TGA plots for compounds **1** (top) and **3** (bottom). The solid curves correspond to the percent weight loss (left *y* axes) and the dashed curves to the heat flow (right *y* axes).

$$Cp^*_2Mo_xW_{6-x}O_{17} + O_2 \xrightarrow{\Delta} 6\ Mo_{x/6}W_{(1-x/6)}O_3 + \text{"}Cp^*_2O\text{"} \quad (2)$$

X-ray Powder Diffraction

As mentioned in the introduction, single-crystal X-ray structures have already been determined for compounds **1** and **4**[51,56] and shown to be isomorphous (monoclinic *C*2/*c*) with very similar unit cell parameters. We therefore considered that the same crystal system may also be adopted by the mixed-metal compounds **2** and **3**. Furthermore, an X-ray powder diffraction study was also reported for compound **1**, as obtained in microcrystalline form by the same condensation process depicted in Equation (1) in aqueous solution, and shown to match with the pattern calculated from the single-crystal data.[51] Thus, we have proceeded to measure powder X-ray diffraction patterns for compounds **2** and **3**. Compound **2** was obtained in sufficient microcrystalline quality to give a well-resolved powder spectrum, which is shown in Figure 3. This pattern was compared with that calculated from the model obtained by changing the M atoms from Mo to W in the known X-ray structure of compound **1**. All measured peaks are accounted for by the model, showing that the sample does not contain any other diffracting phases. All subsequent attempts to refine the atom positions, even when restricted only to the metal atoms, did not lead to convergence. This is probably due to the transmission geometry used for recording the diffracted intensities. Indeed, since it was difficult to synthesize a high quantity of powder (necessary for working in the reflection mode), we used the transmission mode on a sample in a capillary, and the high absorption prevented a good simulation of the diffracted intensities. The diffraction geometry also resulted in high peak asymmetry, as most clearly visible for the most intense peaks at low angles. However, free refinement of the thermal parameters of the metal atoms and of a common thermal parameter for the C and O atoms gave very reasonable values, with R = 5.14, R_p = 17.8, R_{wp} = 17.8 and a Bragg R factor of 13.82. It is notable that refinement of all other possible models corresponding to the metal placement as expected for **1**, **3** and **4** gave unreasonably low (when the W position was modelled by Mo) or high (when the Mo position was

modelled by W) thermal parameters. Figures of these refined structures are shown in the Supporting Information. The *R* factors for the three wrong models were slightly greater (**1**: 6.28%; **3**: 9.04%; **4**: 6.51%) than those for the correct model. Thus, the powder X-ray diffraction experiment provides strong evidence that compound **2** has the same structure previously determined for **1** and **4**, in which Mo occupies solely the inorganic sites and W occupies solely the organometallic sites. The same conclusions concerning the structure and the site selectivity can reasonably be assumed for compound **3**.

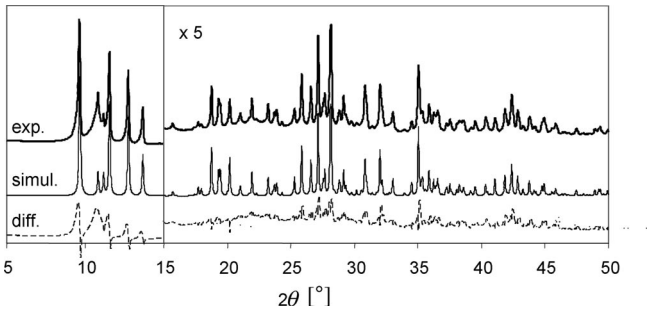

Figure 3. Powder X-ray diffraction patterns for compound **2**. Solid line (top): experimental spectrum; solid line (middle): simulated spectrum; dashed line (bottom): difference.

Conclusions

We have presented here a rational and facile synthesis of organometallic Lindqvist-type polyoxo(group 6 metal) compounds of type $Cp^*_2M_2M'_4O_{17}$ (M = Mo, W). This route, already known for the M = M′ = Mo member (compound **1**), has now been extended to afford a high-yield selective synthesis of the already known M = M′ = W member (compound **4**) and also to prepare the previously unknown mixed-metal systems. Thermal decomposition of these compounds has been shown to yield mixed-metal oxides $Mo_{2/3}W_{1/3}O_3$ and $Mo_{1/3}W_{2/3}O_3$ with an expected homogeneous distribution of the two metals, which may be of interest for the study of the influence of the metal in heterogeneous catalytic as well as in chromogenic applications.

Experimental Section

All experiments were performed in air. Compounds $Cp^*_2Mo_2O_5$ and $Cp^*_2W_2O_5$ were synthesized according to the literature.[48] Water was deionized, and methanol (Carlo Erba, analytical grade) was used as received. Sodium tungstate dihydrate ($Na_2WO_4{\cdot}2H_2O$) and sodium molybdate dihydrate ($Na_2MoO_4{\cdot}2H_2O$) were purchased from Aldrich and used as received. Elemental analyses (C, H and O) were performed by the LCC Analytical Service Laboratory. The IR spectra were recorded on KBr pellets at room temperature with a Mattson Genesis II FTIR spectrometer and the data were processed with WinFirst software. The TGA measurements were carried out with a SDT Q600 V20.9 thermal analyzer. A quantity of each sample was placed into a nickel/platinum alloy crucible and heated at 0.83 K s^{-1} under reconstituted air flow up to 600 K. An empty crucible was used as reference.

$Cp^*_2Mo_6O_{17}$ (1): The synthesis procedure follows that reported previously, except that the latter contains a typographical error in the amount of acid used.[51] Thus, using $Cp^*_2Mo_2O_5$ (27 mg, 5.0×10^{-2} mmol) in MeOH (1.25 mL), $Na_2MoO_4{\cdot}2H_2O$ (48.4 mg, 0.20 mmol) in water (1.25 mL) and a HNO_3 solution (0.4 mL, 0.4 mmol, 1 M) led to 23.5 mg of product (62% yield). The IR spectrum matched that reported previously. $C_{20}H_{30}Mo_6O_{17}$ (1118.08): calcd. C 21.48, H 2.70; found C 21.44, H 2.60. TGA (loss of Cp* and uptake of O): calcd. 22.7%; found 23.1%.

$Cp^*_2W_2Mo_4O_{17}$ (2): $Cp^*_2W_2O_5$ (30 mg, 4.18×10^{-2} mmol) was dissolved in MeOH (2 mL). Separately, $Na_2MoO_4{\cdot}2H_2O$ (40 mg, 0.167 mmol) was dissolved in water (2 mL). The two solutions were mixed without apparent change. A HNO_3 solution (0.75 mL, 0.75 mmol, 1 M) was then slowly added, forcing the immediate formation of a dark yellow precipitate, which became paler yellow after ca. 1 h. After being stirred overnight at room temperature, the solid was filtered, washed with H_2O, then with MeOH (in which it is sparingly soluble) and finally dried at 70 °C (38.5 mg, 71.3% yield). IR (KBr pellets): $\tilde{\nu}$ = 1496 (s), 1442 (s), 1377 (s), 1081 (s), 1024 (sh), 984 (sh), 972 (s), 828 (sh), 801 (s), 785 (sh), 600 (s) cm^{-1}. $C_{20}H_{30}Mo_4O_{17}W_2$ (1293.88): calcd. C 18.56, H 2.34; found C 18.47, H 1.73. TGA (loss of Cp* and uptake of O): calcd. 19.6%; found 19.3%.

$Cp^*_2Mo_2W_4O_{17}$ (3): $Cp^*_2Mo_2O_5$ (54.2 mg, 0.1 mmol) was dissolved in MeOH (2.5 mL). Separately, $Na_2WO_4{\cdot}2H_2O$ (131.9 mg, 0.4 mmol) was dissolved in water (2.5 mL). The two solutions were mixed with no apparent change. A HNO_3 solution (1.8 mL, 1.8 mmol, 1 M) was slowly added, forcing the immediate formation of an bright orange precipitate that darkened with time until green. The mixture was stirred overnight. The solid was filtered and finally dried at 70 °C under vacuum. The powder was then washed with diethyl ether to remove unreacted $Cp^*_2Mo_2O_5$. (yield: 86.5 mg, 15%). IR (KBr pellets): $\tilde{\nu}$ = 1491 (s), 1444 (s), 1376 (s), 1265 (w), 1173 (w), 1093 (w), 972 (s), 920 (sh), 890 (sh), 851 (sh), 809 (s), 767 (sh), 706 (s), 610 (s), 546 (s) cm^{-1}. $C_{20}H_{30}Mo_2O_{17}W_4$ (1469.68): calcd. C 16.34, H 2.06; found C 16.68, H 1.70. TGA (loss of Cp* and uptake of O): calcd. 17.3%; found 19.7%.

$Cp^*_2W_6O_{17}$ (4): $Cp^*_2W_2O_5$ (30 mg, 4.2×10^{-2} mmol) was dissolved in MeOH (2 mL). Separately, $Na_2WO_4{\cdot}2H_2O$ (55 mg, 0.17 mmol) was dissolved in water (1.5 mL). The two solutions were mixed with no apparent change. A HNO_3 solution (0.33 mL, 330 mmol, 1 M) was slowly added, forcing the immediate precipitation of a yellow-white powder. The mixture was stirred for one day, and then the yellow solid was filtered, washed with H_2O, then with MeOH and finally dried at 70 °C under vacuum (46.4 mg, 67.5% yield). IR (KBr pellets): $\tilde{\nu}$ = 1498 (s), 1442 (s), 1376 (s), 996 (sh), 980 (s), 896 (sh), 806 (s), 741 (w), 600 (sh) cm^{-1}. $C_{20}H_{30}O_{17}W_6$ (1645.48): calcd. C 14.59, H 1.83; found C 15.14, H 1.33. TGA (loss of Cp* and uptake of O): calcd. 15.4%; found 16.3%.

X-ray Powder Analyses: The XRD data was collected at room temperature with a theta/theta Panalytical MPdPro powder diffractometer, using Cu-K_α radiation (λ = 0.15406 nm), in transmission mode on a capillary sample. The XRD pattern was recorded with a step width of 0.016 and a counting time of 1000 s step^{-1}. The sample was measured over a 2θ range of $5° \le 2\theta \le 70°$. The indexation of the pattern, the full profile matching and the Rietveld refinement were performed by using the Winplotr interface.[61]

Computational Details: The guess geometries for **I** and **IV** were based on the crystallographically determined structures of **1** and

4,[51,56] by replacing all CH_3 groups by H atoms in the Cp* ligands. From the resulting optimized geometries, starting geometries for **II** and **III** were generated by changing the metal. All optimizations were carried out on isolated gas-phase molecules by using the Gaussian 03 suite of programs[62] with the B3LYP functional, which includes the three-parameter gradient-corrected exchange functional of Becke[63] and the correlation functional of Lee, Yang and Parr.[64,65] The standard 6-31G** basis set was used for the C, H and O atoms, while the CE*P*-31G* basis set[66] was adopted for Mo and W. We found that the commonly used LANL2DZ basis set on the metal atom, tested for system **I**, resulted in greater bond lengths than the CE*P*-31G* basis, with a greater difference relative to the experimental values, most likely because polarization functions were not added to the metal atom basis set. Analytical frequency calculations were also run on the optimized geometries, yielding positive frequencies for all normal modes. The calculated IR spectra shown in Figure 1 were generated from the DFT-generated frequencies and intensities by applying Lorentzian functions and adjusting the linewidth to best fit the experimental spectra.

Supporting Information (see footnote on the first page of this article): Figures of normal vibrational modes, structural models for the X-ray diffraction of compound **2** and TGA plots for compounds **2** and **4**.

Acknowledgments

We are grateful to the Centre National de la Recherche Scientifique and to a binational (France–Turkey) Bosphore programme for funding this research. We also thank the French Embassy in Ankara for financial support of the Ph. D. thesis of G. T.-Ç.

[1] G. Schimanke, M. Martin, J. Kunert, H. Vogel, *Z. Anorg. Allg. Chem.* **2005**, *631*, 1289–1296.
[2] M. V. Landau, L. Vradman, A. Wolfson, P. M. Rao, M. Herskowitz, *C. R. Chim.* **2005**, *8*, 679–691.
[3] G. Mestl, *Top. Catal.* **2006**, *38*, 69–82.
[4] P. Kampe, L. Giebeler, D. Samuelis, J. Kunert, A. Drochner, F. Haass, A. H. Adams, J. Ott, S. Endres, G. Schimanke, T. Buhrmester, M. Martin, H. Fuess, H. Vogel, *Phys. Chem. Chem. Phys.* **2007**, *9*, 3577–3589.
[5] S. Endres, P. Kampe, J. Kunert, A. Drochner, H. Vogel, *Appl. Catal. A* **2007**, *325*, 237–243.
[6] W. A. Goddard, K. Chenoweth, S. Pudar, A. C. T. Van Duin, M. J. Cheng, *Top. Catal.* **2008**, *50*, 2–18.
[7] N. R. Shiju, V. V. Guliants, *Appl. Catal. A* **2009**, *356*, 1–17.
[8] S. H. Baeck, T. F. Jaramillo, D. H. Jeong, E. W. Mcfarland, *Chem. Commun.* **2004**, 390–391.
[9] J. Kunert, A. Drochner, J. Ott, H. Vogel, H. Fuess, *Appl. Catal. A* **2004**, *269*, 53–61.
[10] D. Masure, P. Chaquin, C. Louis, M. Che, M. Fournier, *J. Catal.* **1989**, *119*, 415–425.
[11] N. Mizuno, *Trends Phys. Chem.* **1994**, *4*, 349–362.
[12] T. Kim, A. Burrows, C. J. Kiely, I. E. Wachs, *J. Catal.* **2007**, *246*, 370–381.
[13] P. Gouzerh, A. Proust, *Chem. Rev.* **1998**, *98*, 77–111.
[14] A. Proust, R. Thouvenot, P. Gouzerh, *Chem. Commun.* **2008**, 1837–1852.
[15] R. K. C. Ho, W. G. Klemperer, *J. Am. Chem. Soc.* **1978**, *100*, 6772–6774.
[16] W. G. Klemperer, W. Shum, *J. Chem. Soc., Chem. Commun.* **1979**, 60–61.
[17] R. G. Finke, B. Rapko, P. J. Domaille, *Organometallics* **1986**, *5*, 175–178.
[18] P. Gouzerh, Y. Jeannin, A. Proust, F. Robert, *Angew. Chem. Int. Ed. Engl.* **1989**, *28*, 1363–1364.
[19] A. Proust, P. Gouzerh, F. Robert, *Inorg. Chem.* **1993**, *32*, 5291–5298.
[20] T. Nagata, M. Pohl, H. Weiner, R. G. Finke, *Inorg. Chem.* **1997**, *36*, 1366–1377.
[21] F. Zonnevijlle, M. T. Pope, *J. Am. Chem. Soc.* **1979**, *101*, 2731–2732.
[22] W. H. Knoth, *J. Am. Chem. Soc.* **1979**, *101*, 759–760.
[23] W. H. Knoth, *J. Am. Chem. Soc.* **1979**, *101*, 2211–2213.
[24] P. Judeinstein, C. Deprun, L. Nadjo, *J. Chem. Soc., Dalton Trans.* **1991**, 1991–1997.
[25] N. Ammari, G. Herve, R. Thouvenot, *New J. Chem.* **1991**, *15*, 607–608.
[26] A. Mazeaud, N. Ammari, F. Robert, R. Thouvenot, *Angew. Chem. Int. Ed. Engl.* **1996**, *35*, 1961–1964.
[27] D. Agustin, C. Coelho, A. Mazeaud, P. Herson, A. Proust, R. Thouvenot, *Z. Anorg. Allg. Chem.* **2004**, *630*, 2049–2053.
[28] D. Agustin, J. Dallery, C. Coelho, A. Proust, R. Thouvenot, *J. Organomet. Chem.* **2007**, *692*, 746–754.
[29] J. Li, I. Huth, L. M. Chamoreau, B. Hasenknopf, E. Lacote, S. Thorimbert, M. Malacria, *Angew. Chem. Int. Ed.* **2009**, *48*, 2035–2038.
[30] K. Oshihara, Y. Nakamura, M. Sakuma, W. Ueda, *Catal. Today* **2001**, *71*, 153–159.
[31] A. Dolbecq, F. Secheresse, *Adv. Inorg. Chem.* **2002**, *53*, 1–40.
[32] Y. Hayashi, K. Toriumi, K. Isobe, *J. Am. Chem. Soc.* **1988**, *110*, 3666–3668.
[33] G. Suss-Fink, L. Plasseraud, V. Ferrand, H. Stoeckli-Evans, *Chem. Commun.* **1997**, 1657–1658.
[34] P. Blenkiron, A. J. Carty, S. M. Peng, G. H. Lee, C. J. Su, C. W. Shiu, Y. Chi, *Organometallics* **1997**, *16*, 519–521.
[35] C. W. Shiu, Y. Chi, A. J. Carty, S. M. Peng, G. H. Lee, *Organometallics* **1997**, *16*, 5368–5371.
[36] A. Proust, R. Thouvenot, P. Herson, *J. Chem. Soc., Dalton Trans.* **1999**, 51–55.
[37] G. Suss-Fink, L. Plasseraud, V. Ferrand, S. Stanislas, A. Neels, H. Stoeckli-Evans, M. Henry, G. Laurenczy, R. Roulet, *Polyhedron* **1998**, *17*, 2817–2827.
[38] V. Artero, A. Proust, P. Herson, P. Gouzerh, *Chem. Eur. J.* **2001**, *7*, 3901–3910.
[39] E. Collange, J. Garcia, R. Poli, *New J. Chem.* **2002**, *26*, 1249–1256.
[40] F. Demirhan, J. Gun, O. Lev, A. Modestov, R. Poli, P. Richard, *J. Chem. Soc., Dalton Trans.* **2002**, 2109–2111.
[41] D. Saurenz, F. Demirhan, P. Richard, R. Poli, H. Sitzmann, *Eur. J. Inorg. Chem.* **2002**, 1415–1424.
[42] E. Collange, F. Demirhan, J. Gun, O. Lev, A. Modestov, R. Poli, P. Richard, D. Saurenz in *Perspectives in Organometallic Chemistry*, *Vol. 287* (Ed.: C. G. Screttas), Royal Society of Chemistry, Cambridge, UK, **2003**, pp. 167–182.
[43] F. Demirhan, P. Richard, R. Poli, *Inorg. Chim. Acta* **2003**, *347*, 61–66.
[44] R. Poli, *Chem. Eur. J.* **2004**, *10*, 332–341.
[45] F. Demirhan, G. Taban, M. Baya, C. Dinoi, J.-C. Daran, R. Poli, *J. Organomet. Chem.* **2006**, *691*, 648–654.
[46] F. Demirhan, B. Çagatay, D. Demir, M. Baya, J.-C. Daran, R. Poli, *Eur. J. Inorg. Chem.* **2006**, 757–764.
[47] C. Dinoi, P. Prikhodchenko, F. Demirhan, J. Gun, O. Lev, J.-C. Daran, R. Poli, *J. Organomet. Chem.* **2007**, *692*, 2599–2605.
[48] C. Dinoi, G. Taban, P. Sözen, F. Demirhan, J.-C. Daran, R. Poli, *J. Organomet. Chem.* **2007**, *692*, 3743–3749.
[49] C. Dinoi, P. Sözen, G. Taban, D. Demir, F. Demirhan, P. Prikhodchenko, J. Gun, O. Lev, J.-C. Daran, R. Poli, *Eur. J. Inorg. Chem.* **2007**, 4306–4316.
[50] R. Poli, *Coord. Chem. Rev.* **2008**, *252*, 1592–1612.
[51] E. Collange, L. Metteau, P. Richard, R. Poli, *Polyhedron* **2004**, *23*, 2605–2610.
[52] H. Allcock, E. Bissell, E. Shawl, *Inorg. Chem.* **1973**, *12*, 2963–2968.
[53] C. Garner, N. Howlader, A. Mcphail, R. Miller, K. Onan, F. Mabbs, *J. Chem. Soc., Dalton Trans.* **1978**, 1582–1589.

[54] J. Fuchs, K. F. Jahr, *Z. Naturforsch., Teil B* **1968**, *23*, 1380.
[55] F. Bottomley, J. Chen, *Organometallics* **1992**, *11*, 3404–3411.
[56] J. R. Harper, A. L. Rheingold, *J. Am. Chem. Soc.* **1990**, *112*, 4037–4038.
[57] J.-E. Jee, A. Comas-Vives, C. Dinoi, G. Ujaque, R. Van Eldik, A. Lledós, R. Poli, *Inorg. Chem.* **2007**, *46*, 4103–4113.
[58] C. Rocchiccioli-Deltcheff, M. Fournier, R. Franck, R. Thouvenot, *J. Mol. Struct.* **1984**, *114*, 49–56.
[59] C. Rocchiccioli-Deltcheff, R. Thouvenot, M. Fouassier, *Inorg. Chem.* **1982**, *21*, 30–35.
[60] A. J. Bridgeman, G. Cavigliasso, *Chem. Phys.* **2002**, *279*, 143–159.
[61] T. Roisnel and J. Rodríguez, *WINPLOTR*, http://www.cdifx.univ-rennes1.fr/winplotr/winplotr.htm, **2009**.
[62] M. J. Frisch, G. W. Trucks, H. B. Schlegel, G. E. Scuseria, M. A. Robb, J. R. Cheeseman, J. Montgomery, J. A., T. Vreven, K. N. Kudin, J. C. Burant, J. M. Millam, S. S. Iyengar, J. Tomasi, V. Barone, B. Mennucci, M. Cossi, G. Scalmani, N. Rega, G. A. Petersson, H. Nakatsuji, M. Hada, M. Ehara, K. Toyota, R. Fukuda, J. Hasegawa, M. Ishida, T. Nakajima, Y. Honda, O. Kitao, H. Nakai, M. Klene, X. Li, J. E. Knox, H. P. Hratchian, J. B. Cross, C. Adamo, J. Jaramillo, R. Gomperts, R. E. Stratmann, O. Yazyev, A. J. Austin, R. Cammi, C. Pomelli, J. W. Ochterski, P. Y. Ayala, K. Morokuma, G. A. Voth, P. Salvador, J. J. Dannenberg, V. G. Zakrzewski, S. Dapprich, A. D. Daniels, M. C. Strain, O. Farkas, D. K. Malick, A. D. Rabuck, K. Raghavachari, J. B. Foresman, J. V. Ortiz, Q. Cui, A. G. Baboul, S. Clifford, J. Cioslowski, B. B. Stefanov, G. Liu, A. Liashenko, P. Piskorz, I. Komaromi, R. L. Martin, D. J. Fox, T. Keith, M. A. Al-Laham, C. Y. Peng, A. Nanayakkara, M. Challacombe, P. M. W. Gill, B. Johnson, W. Chen, M. W. Wong, C. Gonzalez and J. A. Pople, *Gaussian 03, Revision D.01*, Gaussian, Inc., Wallingford, CT, **2004**.
[63] A. D. Becke, *J. Chem. Phys.* **1993**, *98*, 5648–5652.
[64] C. T. Lee, W. T. Yang, R. G. Parr, *Phys. Rev. B* **1988**, *37*, 785–789.
[65] B. Miehlich, A. Savin, H. Stoll, H. Preuss, *Chem. Phys. Lett.* **1989**, *157*, 200–206.
[66] W. J. Stevens, M. Krauss, H. Basch, P. G. Jasien, *Can. J. Chem.* **1992**, *70*, 612–630.

Received: July 18, 2009
Published Online: September 25, 2009

